Acta Crystallographica Section F
Structural Biology and Crystallization Communications
ISSN 1744-3091

Escherichia coli tRNA^{Arg} acceptor-stem isoacceptors: comparative crystallization and preliminary X-ray diffraction analysis

André Eichert,[a] Angela Schreiber,[a] Jens P. Fürste,[a] Markus Perbandt,[b] Christian Betzel,[c] Volker A. Erdmann[a] and Charlotte Förster[a]*

[a]Institute of Chemistry and Biochemistry, Free University Berlin, Thielallee 63, 14195 Berlin, Germany, [b]Institute of Biochemistry, Laboratory for Structural Biology of Infection and Inflammation, University of Lübeck, Building 22a, c/o DESY, 22603 Hamburg, Germany, and [c]Institute of Biochemistry and Food Chemistry, University of Hamburg, Notkestrasse 85, Building 22a, c/o DESY, 22603 Hamburg, Germany

Correspondence e-mail: foerster@chemie.fu-berlin.de

Received 4 November 2008
Accepted 10 December 2008

The aminoacylation of tRNA is a crucial step in cellular protein biosynthesis. Recognition of the cognate tRNA by the correct aminoacyl-tRNA synthetase is ensured by tRNA identity elements. In tRNA^{Arg}, the identity elements consist of the anticodon, parts of the D-loop and the discriminator base. The minor groove of the aminoacyl stem interacts with the arginyl-tRNA synthetase. As a consequence of the redundancy of the genetic code, six tRNA^{Arg} isoacceptors exist. In the present work, three different *Escherichia coli* tRNA^{Arg} acceptor-stem helices were crystallized. Two of them, the tRNA^{Arg} microhelices RR-1660 and RR-1662, were examined by X-ray diffraction analysis and diffracted to 1.7 and 1.8 Å resolution, respectively. The tRNA^{Arg} RR-1660 helix crystallized in space group $P1$, with unit-cell parameters a = 26.28, b = 28.92, c = 29.00 Å, α = 105.74, β = 99.01, γ = 97.44°, whereas the tRNA^{Arg} RR-1662 helix crystallized in space group $C2$, with unit-cell parameters a = 33.18, b = 46.16, c = 26.04 Å, β = 101.50°.

1. Introduction

The translation of genetic information is ensured by the correct aminoacylation of tRNAs by their cognate aminoacyl-tRNA synthetases (aaRS). tRNA identity is directed by tRNA determinants, which consist of different sequence and structure motifs. The tRNAs/aaRS systems can be divided into two major groups: class I and class II systems (Eriani *et al.*, 1990).

Class I aaRS recognize complex tRNA identity elements that consist of sequences or nucleotides that are spread over different regions of the tRNA, mostly including the anticodon. In contrast, class II aminoacyl-tRNA synthetases depend on a rather few simple tRNA determinants that are mainly located in the aminoacyl stem of the corresponding tRNAs and may even only consist of a single base pair (Hou & Schimmel, 1988).

Owing to the redundancy of the genetic code, several isoacceptor tRNAs often exist that translate different mRNA codons with the same amino-acid specificity. tRNA isoacceptors that differ in sequence but not in their identity elements are aminoacylated by the same unique synthetase. The corresponding synthetases therefore have to reject noncognate tRNAs on one hand but have to aminoacylate the correct tRNA isoacceptors on the other. The recognition between tRNA and synthetase is a crucial process to ensure accurate protein biosynthesis.

One example of the existence of multiple tRNA isoacceptors is the arginine system. Six different codons exist for arginine and are accompanied by several tRNA^{Arg} isoacceptors. To date, the sequences of five different *Escherichia coli* tRNA^{Arg} species have been identified and published in the tRNA database (Sprinzl & Vassilenko, 2005). The tRNA^{Arg} identity elements have been well investigated. The tRNA^{Arg}/arginyl-tRNA synthetase belongs to the class I system (Eriani *et al.*, 1990) and the tRNA determinants consist of several sequence motifs in different regions of the tRNA. In tRNA^{Arg} they consist of the anticodon, position 20 in the variable loop of the tRNA and the discriminator base at position 73 (McClain *et al.*, 1990; Schulmann & Pelka, 1989; Sprinzl & Vassilenko, 2005). The *Thermus thermophilus* ArgRS (Shimada *et al.*, 2001) and com-

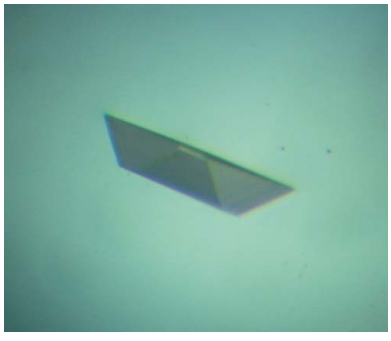

plexes between yeast tRNA^{Arg} and the corresponding ArgRS (Delagoutte *et al.*, 2000) have been crystallized and their X-ray structures have been solved. These structural investigations provided new insights into tRNA^{Arg}–ArgRS interactions and conformations. It was also demonstrated that the minor groove of the tRNA^{Arg} acceptor stem interacts with the synthetase.

Here, we report the crystallization and preliminary X-ray diffraction data of various *E. coli* tRNA^{Arg} acceptor-stem microhelices derived from tRNA^{Arg} 1 (tRNA database ID RR-1660), tRNA^{Arg} 2 (RR-1662) and tRNA^{Arg} 3 (RR-1664) (Sprinzl & Vassilenko, 2005).

We are interested in comparative structural analysis of different tRNA^{Arg} microhelices for the following reasons. Firstly, this system is known to possess at least six tRNA^{Arg} isoacceptors with different sequences in the acceptor stems (Sprinzl & Vassilenko, 2005). Nevertheless, it was shown in the structure of a tRNA^{Arg}–ArgRS complex that the minor groove of the tRNA acceptor stem interacts with the active site of the protein (Delagoutte *et al.*, 2000). We wish to compare the microhelix structures by superposition experiments, as recently peformed with tRNA^{Gly} microhelix structures (Förster *et al.*, 2008). We also plan to perform docking experiments to the synthetase in order to further investigate tRNA^{Arg} acceptor stem–ArgRS binding, as has recently been demonstrated with a tRNA^{Ser} microhelix (Förster *et al.*, 2007). Secondly, we focus on high-resolution X-ray crystallography in order to examine the water molecules surrounding the tRNA. It is well accepted that the hydration of RNA plays an important role within the interacting surfaces and has a special function in RNA owing to the extensive solvent content of the minor groove. This is governed by the specific hydration of the ribose 2′-OH group (Auffinger & Westhof, 1998; Draper, 1999). The study presented here contributes to a general understanding of tRNA microhelix structures (Förster *et al.*, 2008; Limmer *et al.*, 1993; Mueller, Muller *et al.*, 1999; Mueller, Schubel et al., 1999; Ramos & Varani, 1997) and to the tRNA^{Arg} system in particular.

2. Materials and methods

2.1. Crystallization of the *E. coli* tRNA^{Arg} microhelices

All RNA oligonucleotides were purchased from IBA (Göttingen, Germany) and were of HPLC-purification grade. As the commercial RNA synthesis and subsequent HPLC purification of RNA gives high-quality molecules which have been successfully used for crystallization and structure determination in the past (Förster *et al.*, 2007, 2008), no further isolation or purification was applied. We routinely checked RNA-duplex formation by measuring the melting curves (data not shown).

The complementary sequences 5′-GCAUCCG-3′ and 5′-CGGAUGC-3′ belong to the aminoacyl stem of *E. coli* tRNA^{Arg} 1 (RR-1660), oligonucleotides with sequences 5′-GUCCUCU-3′ and 5′-AGGGGAC-3′ correspond to *E. coli* tRNA^{Arg} 2 (RR-1662) and the RNAs with the sequences 5′-GCGCCCG-3′ and 5′-CGGGCGC-3′ represent the *E. coli* tRNA^{Arg} acceptor stem 3 (RR-1664). The concentration of the single RNA strands was determined by alkaline hydrolysis considering the molar extinction coefficients of the single nucleotides and UV spectroscopy as described in Sproat *et al.* (1995).

For formation of the tRNA^{Arg} microhelix duplexes, the corresponding complementary RNA strands were annealed in deionized water pH 5.5 at a concentration of 0.5 m*M*. After heating the mixture to 363 K for 2 min, the RNA oligonucleotides were cooled to room temperature over several hours, allowing the hybridization of the RNA duplexes as demonstrated by melting curves (data not shown). This resulted in the formation of the RNA helices RR-1660, RR-1662 and RR-1664 with molecular weights of 4399, 4400 and 4429 Da, respectively. These duplexes were used in initial crystallization screening experiments.

With all tRNA^{Arg} microhelices initial screening trials were performed with two different nucleic acid screens, which were applied simultaneously. The Natrix Formulation kit (HR2-116) from Hampton Research (California, USA) was used applying the sitting-drop vapour-diffusion technique with CrystalQuick Lp plates from Greiner Bio-One (Germany). 1 µl 0.5 m*M* RNA solution was mixed

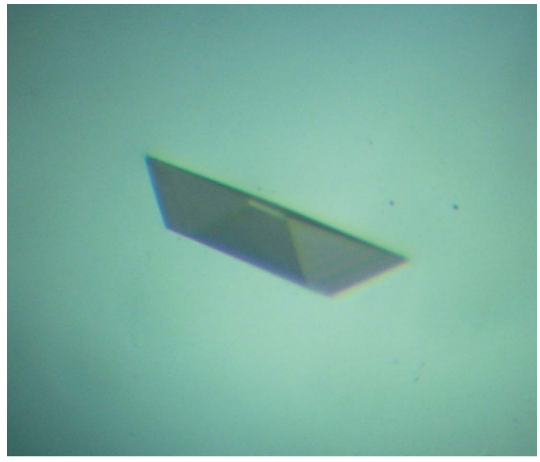

(*a*)

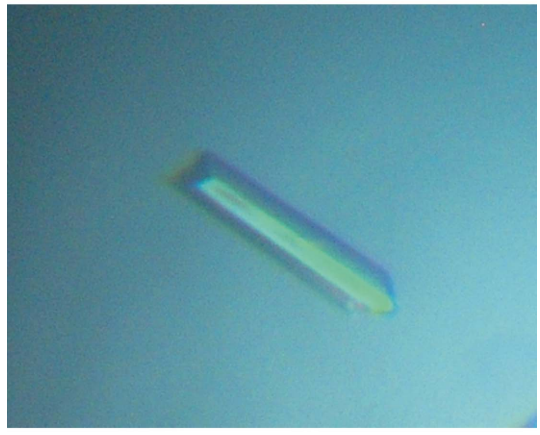

(*b*)

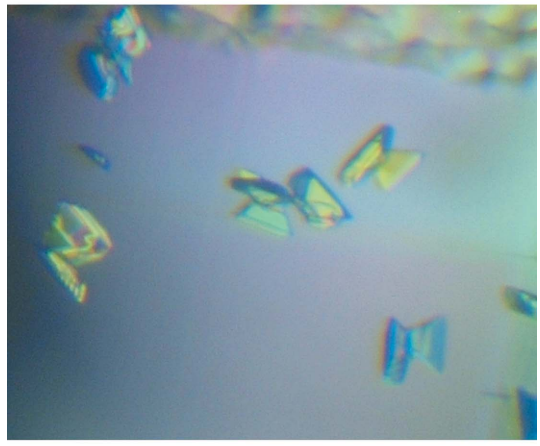

(*c*)

Figure 1
Crystals of the *E. coli* tRNA^{Arg} acceptor-stem microhelices (*a*) RR-1660, (*b*) RR-1662 and (*c*) RR-1664.

Table 1
Data-collection and processing statistics of the *E. coli* tRNA^{Arg} isoacceptor-stem microhelices RR-1660 and RR-1662.

Values in parentheses are for the highest resolution shell.

	tRNA^{Arg} microhelix RR-1660	tRNA^{Arg} microhelix RR-1662
Beamline	Elettra/XRD1 (BL 5.2R)	Elettra/XRD1 (BL 5.2R)
Wavelength (Å)	1.000	1.000
Space group	*P*1	*C*2
Unit-cell parameters (Å,°)	a = 26.28, b = 28.92, c = 29.00, α = 105.74, β = 99.01, γ = 97.44	a = 33.18, b = 46.16, c = 26.04, β = 101.50
Matthews coefficient V_M (Å^3 Da^{-1})	2.34	2.32
RNA duplexes per ASU	2	1
Solvent content† (%)	59.6	59.2
Measured reflections	12812	13900
Unique reflections	7118	3758
Resolution range (Å)	40.0–1.70 (1.73–1.70)	40.0–1.80 (1.83–1.80)
Completeness (%)	95.0 (93.2)	100.00 (100.00)
Multiplicity (%)	1.8 (1.7)	3.7 (3.7)
R_{merge}‡ (%)	3.8 (16.5)	8.6 (25.2)
Average $I/\sigma(I)$	22.2 (1.9)	22.0 (2.2)

† Estimated using the average partial specific volume calculated for RNA by Voss & Gerstein (2005). ‡ $R_{merge} = \sum_{hkl}\sum_i |I_i(hkl) - \langle I(hkl)\rangle| / \sum_{hkl}\sum_i I_i(hkl)$, where $I_i(hkl)$ and $\langle I(hkl)\rangle$ are the observed individual and mean intensities of the reflection with indices *hkl*, respectively, $\sum_i$ is the sum over the individual measurements of a reflection with indices *hkl* and $\sum_{hkl}$ is the sum over all reflections.

with 1 µl reservoir solution. Setups were equilibrated against 80 µl reservoir solution at 294 K. The Nucleic Acid Miniscreen (HR2-118) from Hampton Research (California, USA) was used for parallel screening experiments. In this case, the hanging-drop vapour-diffusion technique was applied using Linbro Plates (ICN Biomedicals Inc., Ohio, USA). Crystallization setups were prepared by mixing 1 µl 0.5 m*M* aqueous RNA solution with 1 µl crystallization solution and the droplet was equilibrated against 1 ml 35%(*v*/*v*) aqueous 2-methyl-2,4-pentanediol (MPD) pH 7.4 at 294 K. For optimizing crystal growth, all setups were performed using the hanging-drop vapour-diffusion technique with the experimental procedure described above.

After optimization of the crystallization conditions, regular crystals of the *E. coli* tRNA^{Arg} 1 (RR-1660) microhelix appeared using 0.5 *M* 2-(*N*-morpholino)ethanesulfonic acid (MES) pH 5.6, 10 m*M* magnesium chloride, 2.0 *M* lithium sulfate at 294 K within 1 d (Fig. 1*a*). The crystals have approximate dimensions of 0.20 × 0.05 × 0.05 mm. Crystals of the second tRNA^{Arg} microhelix (tRNA^{Arg} 2, RR-1662) grew directly using solution No. 20 of the Nucleic Acid Miniscreen, which contained 40 m*M* sodium cacodylate pH 7.0, 12 m*M* spermine tetrahydrochloride, 80 m*M* sodium chloride, 20 m*M* barium chloride, 10%(*v*/*v*) MPD. These crystallization setups were performed at 294 K, which led to regular crystals with maximum dimensions of 0.15 × 0.04 × 0.04 mm within 1 or 2 d (Fig. 1*b*). The tRNA^{Arg} microhelix derived from *E. coli* tRNA^{Arg} 3 (RR-1664) crystallized after optimizing solutions using lithium sulfate as a precipitant, resulting in the following crystallization condition: 0.5 m*M* MES pH 5.6, 100 m*M* magnesium chloride, 1.8 *M* lithium sulfate. Very small crystals appeared at 294 K after 1 or 2 d (Fig. 1*c*).

2.2. Acquisition and processing of the X-ray diffraction data

Prior to X-ray diffraction data collection, all crystals were flash-frozen in liquid nitrogen. The tRNA^{Arg} 1 acceptor-stem crystal (RR-1660) was transferred to the following cryoprotectant solution containing glycerol before freezing: 0.5 *M* MES pH 5.6, 10 m*M* magnesium chloride, 2.0 *M* lithium sulfate and 20%(*v*/*v*) glycerol. The tRNA^{Arg} (RR-1662) microhelix was directly frozen in its crystallization solution, which contained 40 m*M* sodium cacodylate pH 7.0, 12 m*M* spermine tetrahydrochloride, 80 m*M* sodium chloride, 20 m*M* barium chloride and 10%(*v*/*v*) MPD. X-ray diffraction data were recorded from both tRNA^{Arg} microhelix crystals on the Elettra XRD1 (BL 5.2R) beamline in Trieste, Italy at a wavelength of 1.00 Å. For tRNA^{Arg} 1 (RR-1660) a data set was collected from 40 to 1.7 Å resolution at a temperature of 100 K and for tRNA^{Arg} 2 (RR-1662) X-ray diffraction data were acquired from 40 to 1.8 Å resolution. The crystals of the third tRNA^{Arg} microhelix still need to be improved for X-ray diffraction data collection. All crystallographic data were processed using programs from the *HKL*-2000 package (Otwinowski & Minor, 1997). The diffraction data from *E. coli* tRNA^{Arg} microhelices 1 and 2 were analysed for merohedral twinning using the Padilla and Yeates algorithm (Padilla & Yeates, 2003) as implemented in the web server http://nihserver.mbi.ucla.edu/pystats.

3. Results and discussion

3.1. Crystallization

To date, five different *E. coli* tRNA^{Arg} isoacceptor sequences have been deposited in the 'Compilation of tRNA Sequences and Sequences of tRNA Genes' tRNA database (Sprinzl & Vassilenko, 2005). In order to perform a comparative X-ray structure analysis of tRNA^{Arg} acceptor-stem microhelices, we chose three different tRNA sequences derived from the isoacceptors RR-1660, RR-1662 and RR-1664 (Fig. 2). All three RNA duplexes were crystallized and two of them yielded regularly shaped crystals that were suitable for X-ray diffraction data collection.

The crystals of all three microhelices grew relatively rapidly and appeared within 1 or 2 d at 294 K. tRNA^{Arg} RR-1660 microhelix crystals (Fig. 1*a*) grew using lithium sulfate as a precipitant after 24 h as described above. tRNA^{Arg} RR-1662 crystals (Fig. 1*b*) appeared using MPD as a precipitant after 1–2 d. Both crystals were suitable for the acquisition of X-ray diffraction data. Crystals of the third microhelix (RR-1664; Fig. 1*c*) grew in lithium sulfate within 1 or 2 d but were still small and irregular and need to be further improved prior to data collection.

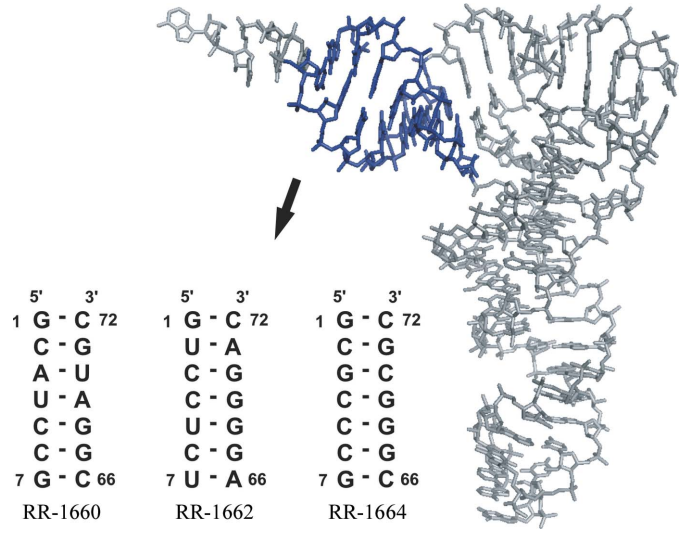

Figure 2
The three-dimensional L-shaped structure of tRNA as determined for yeast tRNA^{Phe} (Shi & Moore, 2000). The *E. coli* tRNA^{Arg} aminoacyl-stem microhelices crystallized in this study are pointed out and represented in blue in the tRNA structure.

3.2. Crystallographic data

The $tRNA^{Arg}$ isoacceptor RR-1660 crystallized in the monoclinic space group $P1$ with two molecules per asymmetric unit and unit-cell parameters a = 26.28, b = 28.92, c = 29.00 Å, α = 105.74, β = 105.74, γ = 97.44°. The Matthews coefficient (V_M) was calculated according to Matthews (1968) and gave a value of 2.34 Å^3 Da^{-1}. This corresponds to a water content of 59.6%, as evaluated by considering the standard atomic values for RNA (Voss & Gerstein, 2005), which reflect a standard solvent content for RNA. Indexing in space groups with higher symmetry failed in this case, so further structure calculations will be performed in space group $P1$ with two RNA molecules per asymmetric unit. A data set was recorded within the 40–1.7 Å resolution range using synchrotron radiation at a wavelength of 1.00 Å and cryogenic cooling. We recorded 12 812 reflections in total, with 7118 unique reflections, corresponding to a multiplicity of 1.8%. The X-ray diffraction data were processed within the resolution range 40–1.70 Å, with an overall R_{merge} of 3.8% and an overall completeness of 95.0% (Table 1).

The second $tRNA^{Arg}$ microhelix RR-1662 crystallizes in space group $C2$, with unit-cell parameters a = 33.18, b = 46.16, c = 26.04 Å, β = 101.50°. The data were recorded from 40 to 1.8 Å resolution with the use of cryogenic cooling and synchrotron radiation of wavelength 1.00 Å. The crystallographic data were recorded and processed within the resolution range 40–1.8 Å. We calculated a Matthews coefficient V_M of 2.32 Å^3 Da^{-1}, which corresponds to a solvent content of 59.2% (Voss & Gerstein, 2005). A total of 13 900 reflections were recorded, with 3758 unique reflections, corresponding to a redundancy of 3.7%. We collected the data with 100.0% completeness (Table 1).

As merohedral disorder is known to occur frequently in small RNA-helix crystals (Mueller, Muller *et al.*, 1999; Mueller, Schubel *et al.*, 1999; Rypniewski *et al.*, 2006), we subjected both data sets to merohedral twinning analysis by applying the Padilla and Yeates algorithm (Padilla & Yeates, 2003) as implemented on the web server at http://nihserver.mbi.ucla.edu/pystats/. According to Padilla & Yeates (2003), analysis of macromolecular X-ray diffraction intensities can be performed by taking the differences between local pairs of reflections. The curve shows the local intensity difference statistics in the presence of anisotropic and pseudo-centering, in which $|L|$ is plotted against $N(|L|)$ with $L = (I_1 - I_2)/(I_1 + I_2)$. The twinning calculations for both $tRNA^{Arg}$ microhelix data sets followed the curve for a theoretically untwinned crystal, so at present we have no indication of merohedral twinning. Currently, molecular-replacement calculations are being applied to solve the structure of the $tRNA^{Arg}$ microhelices RR-1660 and RR-1662 using various RNA helices as search models.

The arginine system belongs to the class I system (Eriani *et al.*, 1990), in which the tRNA identity elements are rather complex and are spread over wide regions of the tRNA. Although the identity elements of $tRNA^{Arg}$ are not located in the acceptor stem, but consist of the anticodon, position 20 in the variable loop and the discriminator base at position 73 (McClain *et al.*, 1990; Schulmann & Pelka, 1989; Sprinzl & Vassilenko, 2005), we are interested in a comparative X-ray structure analysis of $tRNA^{Arg}$ microhelices. In the $tRNA^{Arg}$/arginyl-tRNA synthetase structure solved at 2.2 Å resolution (Delagoutte *et al.*, 2000), the authors discussed an interface between the minor groove of the yeast $tRNA^{Arg}$ acceptor stem and the synthetase. This could be further investigated in the future by superposition experiments using our *E. coli* microhelix structures, as has previously been performed for the $tRNA^{Ser}$/seryl-tRNA synthetase system (Förster *et al.*, 2007). We are also interested in comparing the specific hydration patterns of small tRNA helices, as has been performed for the $tRNA^{Gly}$ system (Förster *et al.*, 2008). The hydration patterns appear to play a role in biological function, since they are the first contact surface within tRNA–protein interactions. These studies contribute to a more detailed understanding of RNA structures and their hydration in general and of the $tRNA^{Arg}$–ArgRS system in particular.

This work was funded within the RiNA network for RNA technologies by the Federal Ministry of Education and Research, the City of Berlin and the European Regional Development Fund. We thank the Fonds der Chemischen Industrie (Verband der Chemischen Industrie eV), the Deutsches Zentrum für Luft- und Raumfahrt (DLR) and the BMBF/VDI-financed BiGRUDI network of the Robert Koch Institute (Berlin) for additional support. We gratefully acknowledge the Elettra synchrotron facility, Trieste for providing beamtime.

References

Auffinger, P. & Westhof, E. (1998). *J. Biomol. Struct. Dyn.* **16**, 693–707.
Delagoutte, B., Moras, D. & Cavarelli, J. (2000). *EMBO J.* **19**, 5599–5610.
Draper, D. E. (1999). *J. Mol. Biol.* **293**, 255–270.
Eriani, G., Delarue, M., Poch, O., Gangloff, J. & Moras, D. (1990). *Nature (London)*, **347**, 203–206.
Förster, C., Brauer, A. B., Fürste, J. P., Betzel, C., Weber, M., Cordes, F. & Erdmann, V. A. (2007). *Biochem. Biophys. Res. Commun.* **362**, 415–418.
Förster, C., Zerressen-Harte, A., Fürste, J. P., Perbandt, M., Betzel, C. & Erdmann, V. A. (2008). *Biochem. Biophys. Res. Commun.* **368**, 1002–1006.
Hou, Y. M. & Schimmel, P. (1988). *Nature (London)*, **333**, 140–145.
Limmer, S., Hofmann, H. P., Ott, G. & Sprinzl, M. (1993). *Proc. Natl Acad. Sci. USA*, **90**, 6199–6202.
Matthews, B. W. (1968). *J. Mol. Biol.* **33**, 491–497.
McClain, W. H., Foss, K., Jenkins, R. A. & Schneider, J. (1990). *Proc. Natl Acad. Sci. USA*, **87**, 9260–9264.
Mueller, U., Muller, Y. A., Herbst-Irmer, R., Sprinzl, M. & Heinemann, U. (1999). *Acta Cryst.* D**55**, 1405–1413.
Mueller, U., Schubel, H., Sprinzl, M. & Heinemann, U. (1999). *RNA*, **5**, 670–677.
Otwinowski, Z. & Minor, W. (1997). *Methods Enzymol.* **276**, 307–326.
Padilla, J. E. & Yeates, T. O. (2003). *Acta Cryst.* D**59**, 1124–1130.
Ramos, A. & Varani, G. (1997). *Nucleic Acids Res.* **25**, 2083–2090.
Rypniewski, W., Vallazza, M., Perbandt, M., Klussmann, S., DeLucas, L. J., Betzel, C. & Erdmann, V. A. (2006). *Acta Cryst.* D**62**, 659–664.
Schulmann, L. H. & Pelka, H. (1989). *Science*, **246**, 1595–1597.
Shi, H. & Moore, P. B. (2000). *RNA*, **6**, 1091–1105.
Shimada, A., Nureki, O., Goto, M., Takahashi, S. & Yokoyama, S. (2001). *Proc. Natl Acad. Sci. USA*, **98**, 13537–13542.
Sprinzl, M. & Vassilenko, K. S. (2005). *Nucleic Acids Res.* **33**, D139–D140.
Sproat, B., Colonna, F., Mullah, B., Tsou, D., Andrus, A., Hampel, A. & Vinayak, R. (1995). *Nucleosides Nucleotides*, **14**, 255–273.
Voss, N. R. & Gerstein, M. (2005). *J. Mol. Biol.* **346**, 477–492.